

## Positive-Projection Monte Carlo Simulation: A New Variational Approach to Strongly Interacting Fermion Systems

S. B. Fahy<sup>(a)</sup> and D. R. Hamann

*AT&T Bell Laboratories, 600 Mountain Avenue, Murray Hill, New Jersey 07974*

(Received 4 May 1990)

We show that very accurate ground-state energies and correlation functions can be obtained from an approximate, variational form of the widely used auxiliary-field simulation method. It is derived by recasting this method as a diffusion problem, and does not exhibit the poor statistical behavior due to vanishing normalization or "sign" common to exact fermion simulations. We give illustrative results for two-dimensional Hubbard models.

PACS numbers: 71.10.+x, 71.45.Nt, 74.20.-z, 75.10.Lp

Monte Carlo simulation is often the only feasible method for understanding the properties of strongly interacting quantum systems. One approach to such simulations is based upon projecting the ground-state wave function  $|\Phi_0\rangle$  from a trial wave function  $|\psi_i\rangle$  by evolving it according to Schrödinger's equation in imaginary time  $\tau$ .<sup>1</sup> The formal solution is

$$|\Phi(\tau)\rangle = e^{-\tau H} |\psi_i\rangle = U(\tau) |\psi_i\rangle, \quad (1)$$

defining the evolution operator  $U$  in terms of the Hamil-

tonian  $H$ . The expectation value of an operator  $A$ ,

$$\langle A \rangle_\tau = \langle \psi_i | U A U | \psi_i \rangle / \langle \psi_i | U U | \psi_i \rangle, \quad (2)$$

thus approaches its ground-state value for large  $\tau$ .

To evaluate such expressions numerically, it is expedient to replace the pair interactions in  $U$  by a functional integral of one-particle operators over a set of  $\tau$ -dependent auxiliary fields  $\mathbf{x}(\tau)$  via the Hubbard-Stratonovich (HS) transformation.<sup>2,3</sup> The resulting expression is

$$\langle A \rangle_\tau = \frac{\int \delta \mathbf{x} G \langle \psi_i | U_P U_{P-1} \cdots U_{P/2-1} A U_{P/2} \cdots U_2 U_1 | \psi_i \rangle}{\int \delta \mathbf{x} G \langle \psi_i | U_P U_{P-1} \cdots U_{P/2-1} U_{P/2} \cdots U_2 U_1 | \psi_i \rangle}, \quad (3)$$

where  $G$  is a Gaussian function of  $\mathbf{x}$ , and  $U_i$  are propagation operators for the discrete time slices  $1, \dots, P$  into which the interval  $(0, 2\tau)$  is typically divided.<sup>3-5</sup> The  $U_i$  contain only one-particle operators (those of the original  $H$  and those representing an  $\mathbf{x}_i$ -dependent external potential), permitting the direct evaluation of the matrix elements in Eq. (3). For fermion systems,  $U_i$  evolves any Slater-determinant state  $|\psi\rangle$  into another Slater determinant, so the proper fermion antisymmetry can be maintained.<sup>3,5</sup>

The major difficulty in evaluating the integrals in Eq. (3) is that the matrix element in the denominator  $D(\mathbf{x}) = \langle \psi_i | U_P \cdots U_1 | \psi_i \rangle$ , which also occurs as a factor of the numerator, can change sign. To evaluate the multidimensional  $\mathbf{x}$  integrals by Monte Carlo methods, importance sampling of  $\mathbf{x}$  based on a positive weight  $G|D|$  must be introduced, which then places a sign factor  $s = D/|D|$  in both integrands.<sup>3</sup> In general, the expectation value of  $s$  is found to vanish exponentially at large  $\tau$ , and statistical errors in the Monte Carlo evaluation of  $\langle A \rangle$  diverge, a phenomenon known as the "sign problem."<sup>6</sup>

$D(\mathbf{x})$  has the form of a determinant in both the ground-state-projection<sup>3,5</sup> and grand-canonical-ensemble methods.<sup>7</sup> We recently analyzed the behavior of  $D$  from "inside," by studying the dynamics of  $|\Phi(\tau)\rangle$  as it evolves from  $|\psi_i\rangle$  under the influence of the random Gaussian fields  $\mathbf{x}$ . Since  $|\psi_i\rangle$  remains a Slater determinant as it propagates through the  $\mathbf{x}$  fields at each time

slice, the Gaussian distribution of all the  $\mathbf{x}$ 's from 0 to  $\tau$  generates a distribution  $f(\psi; \tau)$  of determinants  $|\psi\rangle$ , and

$$|\Phi(\tau)\rangle = \int f(\psi; \tau) |\psi\rangle d\psi, \quad (4)$$

where  $\int d\psi$  represents integration over all normalized Slater determinants.<sup>8</sup> We have shown that  $f$  obeys a diffusion equation with drift and branching,

$$-\frac{\partial f}{\partial \tau} = -\frac{1}{2} D(\psi) f - [\nabla_\psi V_1(\psi)] \cdot \nabla_\psi f + V_2(\psi) f, \quad (5)$$

where the second-order-derivative diffusion operator  $D$ , and the drift and branching potentials,  $V_1$  and  $V_2$ , can be explicitly written in terms of the operators of the initial many-body Hamiltonian.<sup>8</sup> The equation is to be solved with the initial condition  $f(\psi; 0) = \delta(\psi - \psi_i)$ . Equation (3) for  $\langle A \rangle_\tau$  can be reexpressed as

$$\langle A \rangle_\tau = \frac{\int f(\psi; \tau) f(\psi'; \tau) \langle \psi | A | \psi' \rangle d\psi d\psi'}{\int f(\psi; \tau) f(\psi'; \tau) \langle \psi | \psi' \rangle d\psi d\psi'}. \quad (6)$$

The solution of Eq. (5) can, in principle, be expanded in terms of eigenfunctions  $f^i$  and eigenvalues  $\epsilon^i$  of its right-hand side, as

$$f(\psi; \tau) = \sum_i c_i e^{-\epsilon^i \tau} f^i(\psi), \quad (7)$$

where the coefficients  $c_i$  are determined by the initial condition. The manifold of normalized Slater determinants contains both the determinant  $\psi$  and its negative

$-\psi$  as distinct points. We have shown that Eq. (5) is invariant under the parity operator,  $\psi \rightarrow -\psi$ .<sup>8</sup> Given the ordinary diffusion form of Eq. (5), the lowest eigenvalue must belong to an even-parity eigenfunction  $f^+$ , which therefore dominates the sum in Eq. (7) at large  $\tau$ . However, even-parity terms in  $f$  cancel in the integral for the many-body wave function, Eq. (4), and hence in the numerator and denominator of Eq. (6). These *integrals* are dominated by the lowest odd-parity eigenfunction  $f^-$ , while their *integrands* are dominated by  $f^+$ . Statistical evaluation of the integrals requires sufficient accuracy to extract the exponentially small physical contribution. This analysis provides a theoretical basis for the universality of the sign problem, and suggests that it is fundamentally insoluble.<sup>8,9</sup>

The positive-projection (PP) approximation we introduce was motivated by this analysis. Figure 1(a) schematically illustrates a possible  $V_2(\psi)$  potential,  $f^+(\psi)$ , and  $f^-(\psi)$  for a hypothetical one-dimensional  $\psi$  manifold, assuming  $V_1=0$  and a simple  $d^2/d\psi^2$  diffusion term. [A double-well character is strongly evident in the actual examples we have studied, with the basins of attraction near the Hartree-Fock (HF) solutions.] PP consists of supplementing Eq. (5) with the boundary condition  $f(0)=0$ , which is equivalent to setting  $V_2(\psi)=\infty$  for  $\psi < 0$ , as illustrated in Fig. 1(b). The eigenfunction with the lowest eigenvalue is now  $f^-$ . If we did not know the position of the node of  $f^-$  exactly, we would only make a small error if we put it somewhere near the center compared to the double-well separation. Let us denote as  $f^*(\psi;\tau)$  the solution of Eq. (5) subject to the usual initial condition and our PP nodal condition. The  $\langle \psi | \psi' \rangle$  overlap term in the denominator need not be positive. However, the average sign is bounded from below, and usually stays near 1. Equation (6) with  $f^*$  substituted for  $f$  has a variational character, and in particular would give an upper bound for the energy if  $A$  were the Hamiltonian. As with conventional variational calculations, the approximate placement of the  $f^*$  node obviates the possibility of converging to a truly exact solution. Unconstrained projection is always to be preferred where

the rate of sign decay permits an acceptable combination of large  $\tau$  and small statistical errors.

The PP method has a *formal* resemblance to the fixed-node approximation<sup>10</sup> in the Green's-function Monte Carlo (GFMC) method,<sup>11</sup> but the context and physical content are quite different. The naturally dominant term in the unconstrained GFMC method is the boson ground state.<sup>10</sup> The fixed-node approach avoids boson collapse by setting the entire nodal structure of the many-body wave function in ordinary configuration space equal to that of a simple fermion trial function. By contrast, the auxiliary-field method enforces fermion antisymmetry automatically.<sup>3</sup> Even the uncontrolled approximation of neglecting minus signs in Eq. (3),<sup>4</sup> which our analysis shows to be equivalent to approximating  $|f^-|$  by the naturally dominant  $f^+$ ,<sup>8</sup> leads to only small errors in most measured quantities.<sup>4,5</sup> The PP method removes  $f^+$  without imposing any direct constraint on the nodal structure of the many-body wave function, which may adjust with nearly complete freedom according to the Hamiltonian.

The diffusion formulation is more useful for insight than for computation, for which we return to the conventional integration over HS fields using Eq. (3). A practical way to define the PP constraint is to set the nodal surface equal to the hyperplane perpendicular to a "constraint" wave function  $|\Phi_c\rangle$ , which could be one or a small sum of Slater determinants. Heuristically, we expect that the better  $|\Phi_c\rangle$  approximates the ground state, the closer the hyperplane will come to the exact nodal surface of  $f^-$ . If we impose the  $P$  conditions

$$\langle \Phi_c | U_l U_{l-1} \cdots U_2 U_1 | \psi_l \rangle > 0, \quad l=1, \dots, P/2, \quad (8)$$

$$\langle \psi_l | U_P U_{P-1} \cdots U_{l+1} U_l | \Phi_c \rangle > 0, \quad l=P/2+1, \dots, P,$$

on the stochastic process used to sample the HS fields  $\mathbf{x}$ , we achieve the equivalent of setting  $V_2$  in Eq. (2) to  $+\infty$  for all  $\psi$  on the wrong side of the constraint surface. Members of the sample which satisfy Eq. (8) are selected by the usual importance sampling with probability proportional to  $G|D|$  using a hybrid Monte Carlo ap-

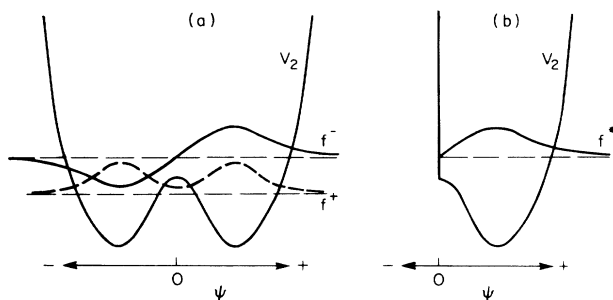


FIG. 1. (a) Schematic illustration of potential  $V_2$  and functions  $f^+$  and  $f^-$  for a one-dimensional  $\psi$  manifold. (b) Solution  $f^*$  with constraint  $V_2 = \infty$  for  $\psi < 0$ .

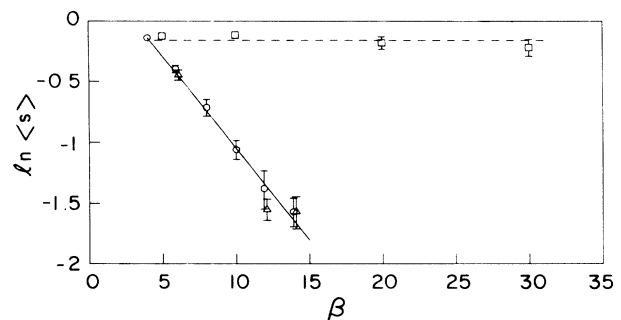


FIG. 2. Natural log of the sign as a function of  $\beta$  for conventional (Ref. 5) (solid) and PP (dashed) simulations of the  $2 \times 2$  three-electron Hubbard model with  $U=4$ .

TABLE I. Average sign  $\langle s \rangle$ , ground-state energy per site  $E$ , exact-diagonalization energy  $E_{\text{diag}}$ , and difference  $\Delta E$  from PP simulations based on  $(0.5-2.0) \times 10^5$  MC samples, for the Hubbard models and parameters indicated. Energies are in units of the hopping parameter  $t$ , constraining states  $|\Phi_c\rangle$  are discussed in the text, and  $\beta = 10t^{-1}$ .

System	$U$	$\Delta\tau$	$ \Phi_c\rangle$	$\langle s \rangle$	$E$	$E_{\text{diag}}$	$\Delta E$
(2x2)-3	4	0.5	1-N	0.85(2)	-1.5980(20)	1.6046	0.0066
(3x3)-8	4	0.5	1-C	0.44(5)	-0.956(21)	-1.0405	0.084
	4	0.5	1-N	0.83(3)	-1.0208(27)		0.0197
	4	0.5	9-N	0.84(2)	-1.0319(31)		0.0086
	8	0.5	1-N	0.88(3)	-0.7528(90)	-0.8093	0.0565
	8	0.25	1-N	0.88(4)	-0.780(10)		0.029
	8	0.25	9-N	0.90(2)	-0.7926(55)		0.0167
(4x4)-14	4	0.5	1-X	0.46(7)	-0.971(11)	-0.9840 <sup>a</sup>	0.013

<sup>a</sup>Reference 13.

proach.<sup>3,5,12</sup> Because of the  $\tau$ -nonlocal nature of the constraint, all the fields are simultaneously updated. In practice, we find that the constraint does not significantly decrease our acceptance rate compared to conventional simulations unless we choose a physically inappropriate  $|\Phi_c\rangle$ , putting the node of  $f^*$  in a high-probability region.

Standard practice in HS simulations is to measure an operator  $A$  at every time slice, since this improves statistics.<sup>3-5</sup> This is not possible here, since the "left" and "right" constraint regions in Eq. (8) cannot overlap. Measuring  $A$  at the midpoint, so that  $f^*(\psi; \tau)$  and  $f^*(\psi'; \tau)$  are sampled identically, ensures that a variational bound is obtained. Alternatively, one could insert additional unconstrained time slices between the constrained regions, and average  $A$  measurements over states evolved by the exact propagators within this central region. This strategy, which is formally similar to the "release node" approach of GFMC,<sup>11</sup> could correct errors caused by an inexact nodal constraint surface. While it reintroduces the sign problem, preliminary tests have shown that moderate-sized central regions do not cause unmanageable sign decay.

To test the PP approach, we selected several two-dimensional Hubbard models with periodic boundary conditions. It is known that the sign problem is worst when the Fermi level falls in a degenerate set of states of the noninteracting system,<sup>6</sup> and we deliberately chose such cases:  $2 \times 2$  with 3 electrons,  $3 \times 3$  with 8, and  $4 \times 4$  with 14. Figure 2 shows the logarithm of the average value of the sign as a function of  $\beta (=2\tau)$  for conventional (solid) and PP (dashed) simulations. It is readily apparent that  $\langle s \rangle$  is exponentially decaying with conventional sampling,<sup>5</sup> and essentially  $\beta$  independent with PP. For the  $\beta=10, U=4$  results shown in Table I, conventional simulations give  $\langle s \rangle$  as 0.01 for  $(4 \times 4)$ -14 (Ref. 6) and  $\sim 0.08$  for  $(3 \times 3)$ -8 (estimated).

The constraining state  $|\Phi_c\rangle$  was most frequently chosen as a single determinant, indicated as "1-X" in Table I, and the same state was used as the trial state  $|\psi_t\rangle$ . To generate these determinants, one-electron

eigenstates were examined in the presence of a pattern of weak "magnetic" potentials, and patterns which split an isolated state above the Fermi level were selected. The patterns for each model are indicated in Fig. 3. The  $N$  pattern for  $(3 \times 3)$ -8 with  $U=4$  gave a significantly lower energy than the  $C$  pattern, indicating the variational improvement of the energy with an improved PP constraint. It also gave a larger  $\langle s \rangle$ , and a better MC acceptance rate. We note that the 1-N  $|\Phi_c\rangle$  is numerically very similar to one of the nine equivalent HF solutions for this problem, thus placing the node of  $f^*$  away from the basin of attraction around this HF state. The sum of nine determinants formed by translating our 1-N state to all lattice sites, denoted 9-N, has the same symmetry as the ground state. Using it for  $|\Phi_c\rangle$  while retaining one such determinant for  $|\psi_t\rangle$  gave even lower energies. For  $U=8$ , decreasing  $\Delta\tau$  to 0.25 to obtain a more accurate representation of the many-body propagator further lowered the energy. This observation emphasizes the role that accurate ground-state projection (large  $\beta$ , small  $\Delta\tau$ ) plays in the PP method, once the nodal constraint is chosen reasonably well. For the  $(4 \times 4)$ -14 test, we chose the pattern labeled  $X$ , whose ground state has equal overlap with states from Néel-like patterns with both possible sublattice magnetizations, and yields a very good energy.

Correlation functions  $\langle c_{i\sigma}^\dagger c_{j\sigma'}^\dagger c_{i\sigma} c_{j\sigma'} \rangle$  provide a more stringent test of the quality of the wave function developed by PP. These are compared with exact diagonalization results in Table II for the  $(2 \times 2)$ -3 and

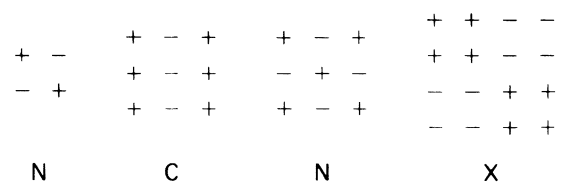


FIG. 3. Patterns of degeneracy-lifting potentials used for  $|\Phi_c\rangle$  in Table I.

TABLE II. Ground-state correlation functions for parallel (p) and antiparallel (a) spins on-site (0) and for first (1) and second (2) neighbors, comparing positive projection (PP) and diagonalization (D) results.  $(2 \times 2)$ -3 has inequivalent first-neighbor correlations. Statistical uncertainty is  $\sim \pm 0.003$ .

System		1p	2p	0a	1a	2a
$(2 \times 2)$ -3	PP	0.238/0.003	0.259	0.142	0.247/0.358	0.253
$\beta=20$	D	0.256/0.001	0.243	0.150	0.235/0.350	0.265
$(3 \times 3)$ -8	PP	0.258	0.408	0.154	0.481	0.369
$\beta=10$	D	0.261	0.406	0.166	0.476	0.371

$(3 \times 3)$ -8 models with  $U=4$ . The  $(2 \times 2)$ -3 model has a pair of degenerate ground states, and a  $2-N$  translated  $|\Phi_c\rangle$  was used to favor a particular broken-symmetry combination. (Nearest-neighbor correlations are inequivalent in the two lattice directions, and two numbers are given in the table.) Different linear combinations of the ground-state pair change all the calculated values, and the difficulty of projecting out a particular combination prevents even better agreement. For  $(3 \times 3)$ -8, the ground state is nondegenerate, although excited states of different symmetry lie within 0.04 hopping-parameter unit. Using the  $9-N$   $|\Phi_c\rangle$  with the correct symmetry contributes to isolating the ground state. While only  $\Delta\tau=0.25$  results are reported here, preliminary examination of extrapolation to  $\Delta\tau=0$  indicates quadratic convergence to the exact result within statistical error.

In summary, we have introduced a variational auxiliary-field quantum Monte Carlo method for fermions which does not exhibit the problem of the exponentially vanishing normalization or "sign." Our analysis in terms of the equivalent diffusion equation shows that the results would be exact if a simple nodal surface were chosen correctly. This analysis and our numerical examples show that excellent ground-state energies and correlation functions can be obtained even without an exact understanding of this surface. There is, of course, no guarantee that PP will give superior results, in any particular case, to a conventional variational calculation with a cleverly chosen wave function. We anticipate, however, that the PP approach should be of considerable advantage in extracting properties of simple models in "problem" cases, and in extending auxiliary-field methods to atoms, molecules, and real materials.

<sup>(a)</sup>Present address: Department of Physics, University of Michigan, Ann Arbor, MI 48109-1120.

<sup>1</sup>N. Metropolis and S. Ulam, *J. Amer. Stat. Assoc.* **44**, 335 (1949).

<sup>2</sup>J. Hubbard, *Phys. Rev. Lett.* **3**, 77 (1959); R. L. Stratonovich, *Dokl. Akad. Nauk. SSSR* **115**, 1097 (1957) [*Sov. Phys. Dokl.* **2**, 416 (1957)].

<sup>3</sup>G. Sugiyama and S. E. Koonin, *Ann. Phys. (N.Y.)* **168**, 1 (1986).

<sup>4</sup>S. Sorella, E. Tosatti, S. Baroni, R. Car, and M. Parrinello, *Int. J. Mod. Phys. B* **1**, 993 (1988); S. Sorella, S. Baroni, R. Car, and M. Parrinello, *Europhys. Lett.* **8**, 663 (1989).

<sup>5</sup>D. R. Hamann and S. B. Fahy, *Phys. Rev. B* **41**, 11352 (1990).

<sup>6</sup>E. Y. Loh, Jr., J. E. Gubernatis, R. T. Scalettar, S. R. White, D. J. Scalapino, and R. L. Sugar, *Phys. Rev. B* **41**, 9301 (1990).

<sup>7</sup>R. Blankenbecler, D. J. Scalapino, and R. L. Sugar, *Phys. Rev. D* **24**, 2278 (1981).

<sup>8</sup>S. B. Fahy and D. R. Hamann, *Phys. Rev. B* **43**, 765 (1991).

<sup>9</sup>Special symmetries of the Hamiltonian can cause the diffusion operator to vanish on a surface separating  $\psi$  and  $-\psi$ , in which case  $f^+$  and  $f^-$  can be degenerate, and the "sign problem" can disappear, as in the half-filled Hubbard model.

<sup>10</sup>P. J. Reynolds, D. M. Ceperley, B. J. Alder, and W. A. Lester, *J. Chem. Phys.* **77**, 5593 (1982).

<sup>11</sup>D. M. Ceperley and M. H. Kalos, in *Monte Carlo Methods in Statistical Physics*, edited by K. Binder (Springer, Berlin, 1986), 2nd ed, p. 145.

<sup>12</sup>S. Duane, A. D. Kennedy, B. J. Pendleton, and D. Roweth, *Phys. Lett. B* **195**, 216 (1987); R. T. Scalettar, D. J. Scalapino, and R. L. Sugar, *Phys. Rev. B* **34**, 7911 (1986).

<sup>13</sup>A. Parola, S. Sorella, S. Baroni, M. Parrinello, and E. Tosatti, *Int. J. Mod. Phys. B* **3**, 1865 (1989).